

# DEPTH-PROFILING OF THE RESIDUAL ACTIVITY INDUCED BY HIGH-ENERGY URANIUM IONS IN THIN STAINLESS STEEL TARGET\*

I. Strasik<sup>#</sup>, GSI Helmholtzzentrum für Schwerionenforschung, Planckstrasse 1, 64291 Darmstadt, Germany, on leave from FEI STU Bratislava, Slovak Republic

E. Mustafin, E. Floch, T. Seidl, A. Plotnikov, E. Schubert, A. Smolyakov, GSI Helmholtzzentrum für Schwerionenforschung, Planckstrasse 1, 64291 Darmstadt, Germany

## Abstract

In the frame of the FAIR project irradiation test of superconducting magnet components was performed at GSI Darmstadt in May 2008. As a part of the experiment stainless steel samples were irradiated by 1 GeV/u  $^{238}\text{U}$  ions. In contrast to the previous experimental studies performed with thick cylindrical samples, the target was a thin plate irradiated at small angle. The target was constituted as a set of individual foils. This stacked-foil target configuration was foreseen for depth-profiling of residual activity. Gamma-ray spectroscopy was used as the main analytical technique. The isotopes with dominating contribution to the residual activity induced in the samples were identified and their contributions were quantified. Depth-profiling of the residual activity of all identified isotopes was performed by measurements of the individual target foils. The characteristic shape of the depth-profiles for the products of target activation and projectile fragments was found and described. Monte Carlo code FLUKA was used for simulations of the residual activity and for estimation of the number of ions delivered to the target and their distribution. The measured data are relevant for assessment of radiation situation at high-energy accelerators during the “hands-on” maintenance as well for assessment of the tolerable beam-losses.

## INTRODUCTION

In recent years, the number of high-energy hadron accelerator facilities in operation, being commissioned, designed or planned has grown-up. Their parameters such as the beam energy, beam currents and intensities has significantly increased and giving rise to new accelerator structure activation and radiation shielding aspects and problems. Residual activity induced in an accelerator structure generally depends on the primary beam losses (amount, energy and mass) as well as on the irradiated material [1] and may become a main source of exposure to personnel and a serious access-restriction for “hands-on” maintenance [2]. In the frame of the FAIR project (Facility for Antiproton and Ion Research) [3], extensive experimental studies [4, 5] and computer simulations [6-9] of the residual activity induced by high-energy heavy-ions in copper and stainless steel were performed at GSI Darmstadt. Copper and stainless steel have been chosen as the representatives of the most common materials for accelerator structures.

The computer simulations can be performed for several ion species and various targets, but the experiments have been so far focused mostly on cylindrical targets irradiated by uranium ions [4, 5]. In contrast to the computer simulations, activation experiments are much more demanding from the beam availability as well as analysis of the irradiated samples. It is practically impossible to carry out irradiation experiments for all primary ions, beam energies and targets of interest. The computer simulations are the only tool to provide this information. Various simulation codes like FLUKA [10], SHIELD [11], MARS [12] etc., are available. However, the computer simulations must be verified by experimental data and more check-points are necessary to validate the codes. That is why the irradiation experiments with cylindrical targets have recently been completed by another experiment with thin stainless steel target irradiated by 1 GeV/u uranium ions. Such kind of target represents thin accelerator structures like a beam pipe. The irradiated target were analysed by gamma-ray spectroscopy and depth-profiling of the partial residual activities of all identified isotopes was performed by measuring the activities of individual target foils.

The activation process is very complex. This is true especially for activation induced by heavy-ion beams. The radioactive nuclides are produced by nuclear reactions induced by primary ions (projectiles) as well as by secondary particles, mostly neutrons and protons, generated by interaction of the primary beam with the target material. On top of that, the projectiles are fragmented into many radioactive projectile-fragments that remain implanted in the target. However, their contribution to the total residual activity is negligible for high-energy projectiles [4, 5].

A summary of the radio-nuclides identified in common materials for accelerator structures irradiated by high energy charged particles is presented in Ref. [13]. Understanding of the activation process provides fundamental information that can be used in two ways: (1) to specify the tolerable beam losses in the machine and (2) to optimize the construction materials. The beam-losses distributed uniformly along the beam line on the level of 1 W/m (equivalent to  $6.24 \times 10^9$  1 GeV protons/m/s) are presently accepted for high-energy proton machines as a threshold for “hands on” maintenance [14]. Tolerances for heavy-ion accelerators can then be specified by scaling the 1 W/m criterion for proton machines [6, 7, 15]. However, the scaling factors have to be obtained again by computer simulations, which

\*Work is partially supported by project VEGA 1/0129/09.  
<sup>#</sup>i.strasik@gsi.de

brings back the necessity to validate the simulation codes and to collect experimental data.

## EXPERIMENT AND METHOD

### Target Configuration and Irradiation Conditions

Target configuration is shown in Figure 1. The target was a plate with 1 mm of thickness  $\times$  50 mm of width  $\times$  150 mm of length. The target was assembled from twenty individual foils with 0.2 mm of thickness  $\times$  50 mm of width  $\times$  40 or 30 mm of length. The target was divided into five layers (A, B, C, D and E) and four segments (1, 2, 3 and 4). The stacked-foil target configuration was foreseen for depth profiling of residual activity. The target material was austenitic Cr-Ni stainless steel (density of  $7.9 \text{ g/cm}^3$ ) contained C (max 0.07 %), Mn (max 2.0 %), P (max 0.045 %), Si (max 1.0 %), Cr (17–19 %), Ni (8.5–10.5 %), N (max 0.1 %) and S (max 0.03 %) in addition to iron. Range of the primary ions was estimated by computer codes ATIMA [16], SRIM [17] and FLUKA [10] (Tab. 1). Detailed experimental and simulation study of the range of high-energy uranium ions in copper and stainless steel is presented in Ref. [18].

Table 1: Range of 1 GeV/u  $^{238}\text{U}$  Ions in Stainless Steel

Computer code	ATIMA	SRIM	FLUKA
Range [mm]	$15.21 \pm 0.01$	$16.70 \pm 0.59$	$16.06 \pm 0.24$

For the target irradiation the 1 GeV/u  $^{238}\text{U}$  beam from SIS-18 synchrotron at GSI-Darmstadt was used. Irradiation time was 30 minutes. The beam spot-size was

about 2 cm in horizontal plane and 1 cm in vertical plane (checked visually on a scintillation screen before irradiation and measured by a profile-meter). The beam profile was approximately Gaussian according to the profile-meter. The glancing angle between the incident beam and surface of the target was about 2 degrees (see Fig. 1). The beam intensity was monitored by a current transformer. Total number of ions registered by current transformer was  $1.07 \times 10^{12}$ , but only a part of the beam hit the target.

## RESIDUAL ACTIVITIES

### Isotope Identification and Activity Measurement

Results of isotope identification and their partial activities are summarized in Table 2. Partial activity represents the activity of each isotope with respect to the total target activity corresponding to the sum of all isotopes. The isotope identification was based on the energy and abundance of the gamma lines, half-life of the isotopes as well as on the experience from the previous experiments [4, 5]. The isotope characteristics were taken from the WWW Table of Radioactive Isotopes [19]. Half-life of the isotopes in Table 2 ranges from 58.6 h ( $^{44\text{m}}\text{Sc}$ ) up to 2.6 y ( $^{22}\text{Na}$ ). For all identified isotopes, the activity for each foil was obtained from the peak-net-areas (PNA) calculated by Genie2000. The measured activity was then extrapolated backwards in time to the end of the irradiation using the characteristic decay constant of a given isotope. Finally, the partial activity for each foil was summed-up to obtain the partial activity of each isotope induced in the whole target.

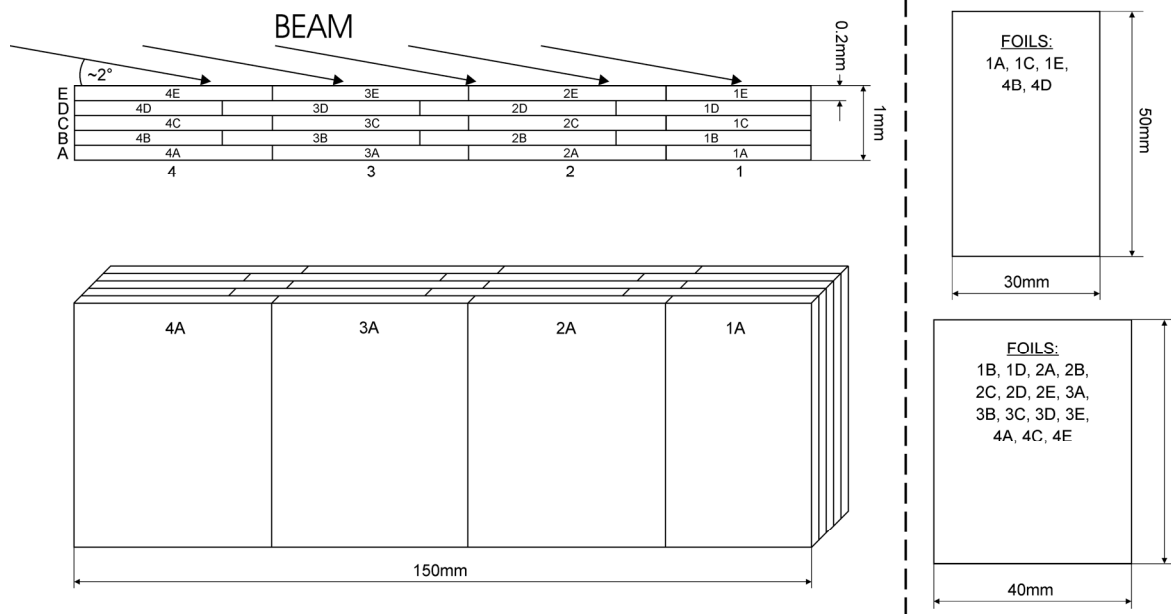


Figure 1: Target configuration and experimental setup. On the left are the parameters of the full-assembly target and on the right are the parameters of individual target foils. The foils are marked by numbers 1, 2, 3 and 4 (segments) and by characters A, B, C, D and E (layers).

Table 2: Identified Isotopes and their Activities

Isotope	Energy [keV]	A <sub>1</sub> [Bq]	σ <sub>1</sub> [%]	A <sub>2</sub> [Bq]	σ <sub>2</sub> [%]
<sup>7</sup> Be	477.6	3.04E+2	2.14	3.25E+2	2.32
<sup>22</sup> Na	1274.5	6.06E+0	6.75	4.71E+0	5.95
<sup>44m</sup> Sc	271.1	8.30E+3	1.37	below MDA	
<sup>46</sup> Sc	889.3	3.18E+2	0.50	3.16E+2	0.56
<sup>47</sup> Sc	159.4	4.38E+3	1.72	below MDA	
<sup>48</sup> V	983.5	3.23E+3	0.30	3.21E+3	0.73
<sup>51</sup> Cr	320.1	4.55E+3	0.38	4.59E+3	0.67
<sup>52</sup> Mn	935.5	4.65E+3	0.45	below MDA	
<sup>54</sup> Mn	834.8	3.09E+2	0.48	3.06E+2	0.46
<sup>56</sup> Co	1238.3	1.49E+2	0.99	1.57E+2	0.81
<sup>57</sup> Co	122.1	8.12E+1	1.73	8.14E+1	1.69
<sup>58</sup> Co	810.8	1.35E+2	0.85	1.22E+2	0.96
<sup>89</sup> Zr	908.9	-	-	-	-
<sup>95</sup> Zr	756.7	2.23E+1	6.53	2.07E+1	5.84
<sup>99</sup> Mo	140.5	6.03E+2	2.74	below MDA	
<sup>103</sup> Ru	497.1	5.49E+1	1.61	4.68E+1	2.60
<sup>121</sup> Te	573.1	1.59E+1	4.44	below MDA	
<sup>126</sup> Sb	414.8	1.71E+1	7.05	below MDA	
<sup>127</sup> Xe	202.9	1.60E+1	4.14	1.67E+1	7.43
<sup>131</sup> Ba	216.1	7.72E+1	5.64	below MDA	
<sup>131</sup> I	364.5	9.47E+1	3.16	below MDA	
<sup>141</sup> Ce	145.4	1.80E+1	4.90	1.68E+1	9.28
<sup>149</sup> Gd	149.7	3.25E+1	5.28	below MDA	
<sup>206</sup> Bi	803.1	4.37E+1	4.94	below MDA	
<sup>237</sup> U	208.0	1.66E+3	0.85	below MDA	

A<sub>1</sub>, A<sub>2</sub> – activity, σ<sub>1</sub>, σ<sub>2</sub> – one standard deviation. Subscript “1” and subscript “2” is related to the spectra measured 8 – 28 and 66 – 91 days after the end irradiation, respectively.

Generally, the activation products have several energy lines in the spectra but only the most pronounced lines or lines without an interference with the same or close energy lines of other isotopes were chosen for activity determination. Some isotopes that could be quantified in the early-measured spectra could not be quantified in the later measured spectra, because they decayed below minimum detectable activity (MDA) level. Determination of the activity of <sup>89</sup>Zr was not possible because its activity decreased below minimum detectable activity before the measurement of all discs was completed.

In the previous experiments performed with cylindrical targets irradiated by uranium beam [4, 5], on the basis of supporting information gained from depth-profiles two

types of isotopes could clearly be distinguished: (1) products of target activation and (2) projectile fragments. Mass number of the target activation products ranged from 7 (<sup>7</sup>Be) up to 58 (<sup>58</sup>Co), whereas mass number of the projectile fragments ranged from 89 (<sup>89</sup>Zr) up to 237 (<sup>237</sup>U).

Table 2 indicates also partial RMS uncertainties of activities. The accuracy of the presented data is influenced by accuracy of the net-peak-areas and accuracy of the efficiency calibration of the detector. These two contributions are summed-up quadratically for each measured foil.

### Depth Profiles of the Residual Activity

Depth-profile is the distribution of the activity as a function of depth in layers A, B, C, D and E of the target. The activity contributions for each foil of the pertinent layer were summed-up in order to get the overall activity of the isotope in the layer (e.g. activity of the foils 1A + 2A + 3A + 4A = activity in the layer A). It was found out in previous experiments [4, 5] that the profiles of the target activation products start at the sample surface and extend deeply beyond the range of primary ions. This is mainly due to large amount of secondary particles that have the range much longer compared to the range of the primary ions. In contrast to that, the depth-profiles of projectile fragments show no signal upstream of the range of primary ions. The profiles start at the range and occupy a region beyond the range from about few mm up to few cm depending on the mass of the fragment. The fragments with mass very close to the mass of the original projectile – <sup>206</sup>Bi and, in particular, <sup>237</sup>U – occupy a thin region well correlated to the range of primary ions (<sup>238</sup>U).

Figures 2, 3 and 4 present a typical depth-profile for target activation product (<sup>52</sup>Mn), light projectile fragment (<sup>99</sup>Mo) and fragment with mass very close to the mass of the primary ion (<sup>237</sup>U), respectively. It can be seen in Fig. 2 that the target activation products have rather flat depth profiles. The depth profiles of the light fragments are characterized by a smooth peak in central layer C and comparatively lower values (more than factor of 2) in outer layers A and E (see Fig. 3). In contrast to the profiles of target activation products, the fragments with mass very close to the mass of the primary ion have a high maximum in central layer C and zero values in outer layers A and E (see Fig. 4). The profiles of the target activation products especially the high level of the activity in outer layers A and E compared to the profiles of the projectile fragments indicate strong scattering of secondary particles such as neutrons and protons causing the activation. The distribution of the <sup>237</sup>U closely correlates to the distribution of primary particles because the <sup>237</sup>U ions have almost the same depth profile as <sup>238</sup>U.

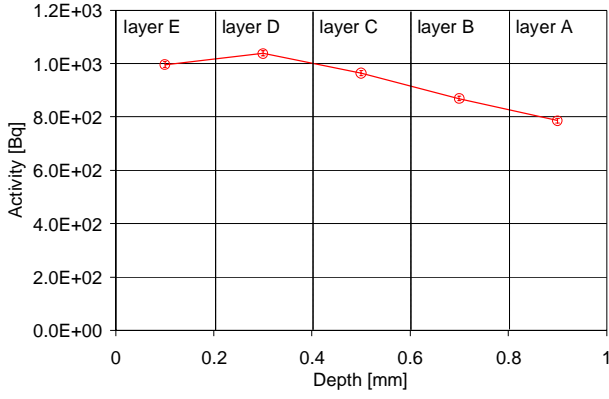


Figure 2: Depth profile of  $^{52}\text{Mn}$ .

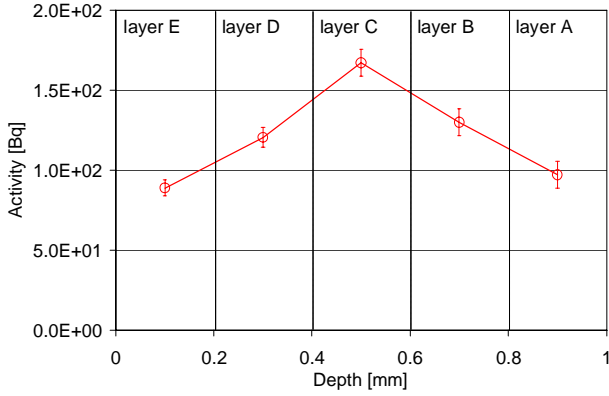


Figure 3: Depth profile of  $^{99}\text{Mo}$ .

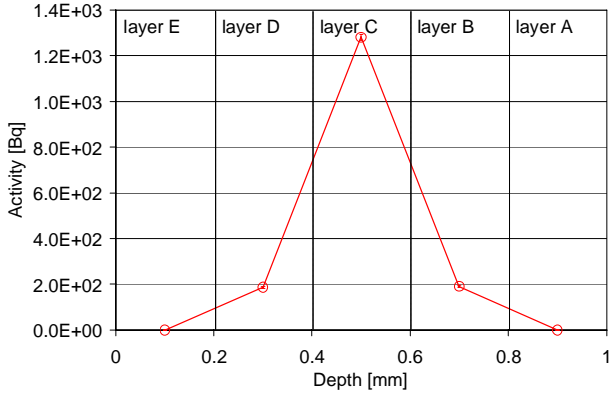


Figure 4: Depth profile of  $^{237}\text{U}$ .

## DISTRIBUTION OF PRIMARY IONS

Monte Carlo particle transport code FLUKA was used for estimation of the number of ions delivered to the target and their distribution because the target was irradiated only by a part of the beam. In the simulation model the same experimental target configuration was applied and glancing angle between the incident beam and surface of the target was 2 degrees (see Fig. 5). The distribution of the beam particles in simulation model was assumed to be uniform. The width of the beam cross-

section in the plane parallel to the target surface was 10 mm across and 30 mm along to the target length (150 mm). Five independent irradiations were simulated for five different position of the beam from beginning up to the end along the target length (see Fig. 5).

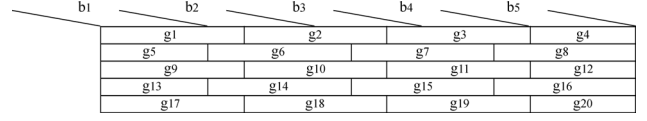


Figure 5: Model of the simulation.

The partial activities of each isotope in twenty foils ( $g_1, \dots, g_{20}$ ) were calculated for five beam positions. The beam distribution was calculated using the formula:

$$\left( \sum_{j=1}^5 g_{ij} b_j - d_i \right) = \delta_i \text{ for } i = 1, 2, \dots, 20 \quad (1)$$

Where  $g_{ij}$  is the activity per one incident ion [Bq/ion] in foil  $i$  for beam position  $j$  calculated by FLUKA,  $b_j$  is number of ions delivered to the target for beam position  $j$  and  $d_i$  is the experimentally measured activity [Bq] in foil  $i$ . The solution of Eq. 1 and unknown values of  $b_j$  were sought as follows:

$$\varphi(b) = \sum_{i=1}^{20} \delta_i^2 = \sum_{i=1}^{20} \left( \sum_{j=1}^5 g_{ij} b_j - d_i \right)^2 \quad (2)$$

$$\frac{\partial \varphi}{\partial b_k} = \sum_{i=1}^{20} \frac{\partial \delta_i^2}{\partial b_k} = \sum_{i=1}^{20} 2g_{ik} \left( \sum_{j=1}^5 g_{ij} b_j - d_i \right) = 0 \quad (3)$$

for  $k = 1, 2, 3, 4, 5$

$$\sum_{j=1}^5 \left( b_j \sum_{i=1}^{20} g_{ik} g_{ij} - \sum_{i=1}^{20} g_{ik} d_i \right) = 0 \quad (4)$$

$$\sum_{i=1}^{20} g_{ik} g_{ij} = G_{kj} \quad \sum_{i=1}^{20} g_{ik} d_i = D_k \quad (5)$$

for  $k = 1, 2, 3, 4, 5$

$$\sum_{j=1}^5 (G_{kj} b_j - D_k) = 0 \quad (6)$$

for  $k = 1, 2, 3, 4, 5$ .

Finally we get the matrix:

$$\begin{aligned}
 & j=1: \quad j=2: \quad j=3: \quad j=4: \quad j=5: \\
 k=1: & G_{11}b_1 + G_{12}b_2 + G_{13}b_3 + G_{14}b_4 + G_{15}b_5 - 5 \times D_1 = 0 \\
 k=2: & G_{21}b_1 + G_{22}b_2 + G_{23}b_3 + G_{24}b_4 + G_{25}b_5 - 5 \times D_2 = 0 \\
 k=3: & G_{31}b_1 + G_{32}b_2 + G_{33}b_3 + G_{34}b_4 + G_{35}b_5 - 5 \times D_3 = 0 \\
 k=4: & G_{41}b_1 + G_{42}b_2 + G_{43}b_3 + G_{44}b_4 + G_{45}b_5 - 5 \times D_4 = 0 \\
 k=5: & G_{51}b_1 + G_{52}b_2 + G_{53}b_3 + G_{54}b_4 + G_{55}b_5 - 5 \times D_5 = 0
 \end{aligned}$$

The distribution of the beam particles ( $b_1, b_2, b_3, b_4$  and  $b_5$ ) was calculated for the activity of the  $^{51}\text{Cr}$ ,  $^{54}\text{Mn}$ ,  $^{99}\text{Mo}$ ,  $^{127}\text{Xe}$  and  $^{238}\text{U}$ . The matrix was solved by Cramer rule and because the matrix is symmetric also by Cholesky decomposition. However results of the calculation showed that our approach failed because the negative values of the number of particles and big inaccuracy of the data were obtained. The reason could be that the calculated results using this method are strongly influenced by the inaccuracy of input data. It must be stressed that the discrepancies between measured and calculated values for individual isotopes induced in stainless steel target irradiated by 1 GeV/u  $^{238}\text{U}$  ions vary from factor of 0.19 to 6.23 [7].

## CONCLUSIONS

Partial residual activities of the isotopes and their depth profiles in stainless steel target irradiated by 1 GeV/u  $^{238}\text{U}$  beam were measured using a gamma-ray spectroscopy analysis of the stacked-foils target. The isotopes that dominate the residual activity from few days to several weeks after the end of irradiation were identified and their partial activities were quantified. The characteristic shape of the depth-profiles for target activation products and projectile fragments was found and described. The target activation products are present in all layers of the target in similar quantities. Such kind of activation is caused by neutrons, protons and lighter fragments. Projectile fragments have a maximum in the centre of the target and their activity in outer layers of the target decreases with increasing mass of the isotope. Experimental results and simulations performed with FLUKA code were used to calculate the distribution of the beam particles delivered to the target. However, our approach failed to give meaningful results of the number and distribution of the incident beam particles on the target surface, hence the method of the calculation must be improved.

## REFERENCES

- [1] A.H. Sullivan, "A Guide to Radiation and Radioactivity Levels Near High Energy Particle Accelerators", Nuclear Technology Publishing, Ashford, Kent, United Kingdom (1992).
- [2] E. Mauro and M. Silari, "Radiation Protection Studies for a High-power 160 MeV Proton Linac" Nucl. Instr. and Meth. in Phys. Res. A, (2009) article in press.
- [3] P. Spiller, G. Franchetti, "The FAIR Accelerator Project at GSI", Nucl. Instr. and Meth. in Phys. Res. A 561 (2006) 305.
- [4] A. Fertman, E. Mustafin, R. Hincă et al., "First Results of an Experimental Study of the Residual Activity Induced by High-Energy Uranium Ions in Steel and Copper", Nucl. Instr. and Meth. in Phys. Res. B 260 (2007) 579.
- [5] I. Strasik, E. Mustafin, A. Fertman et al., "Experimental Study of the Residual Activity Induced by 950 MeV/u Uranium Ions in Stainless Steel and Copper", Nucl. Instr. and Meth. in Phys. Res. B 266 (2008) 3443.
- [6] I. Strasik, E. Kozlova, E. Mustafin et al., "Simulation of the Residual Activity Induced by High-Energy Heavy Ions", Nuclear Technology 168 (2009), article in press.
- [7] I. Strasik, E. Mustafin, E. Kozlova et al., "Residual Activity Induced by High-Energy Heavy Ions in Stainless Steel and Copper", EPAC08, Genoa, Italy, June 2008, p. 3551 (2008).
- [8] E. Kozlova, H. Weick, B. Achenbach et al., "Layout of the Super-FRS Target Hall", Nucl. Instr. and Meth. in Phys. Res. B 266 (2008) 4275.
- [9] H. Iwase, H. Weick, T. Radon et al., "Calculation of activation and dose spatial distributions induced by high intensity uranium beams at the Super-FRS fragment separator at FAIR", Nucl. Instr. and Meth. in Phys. Res. A 562 (2006) 972.
- [10] A. Fasso, A. Ferrari, J. Ranft et al., "FLUKA: a Multi-Particle Transport Code", CERN-2005-10 (2005), INFN/TC\_05/11, SLAC-R-773.
- [11] A.V. Dementyev, N.M. Sobolevsky, "SHIELD - Universal Monte Carlo Hadron Transport Code: Scope and Applications", Radiation Measurements 30 (1999) 553.
- [12] <http://www-ap.fnal.gov/MARS/>
- [13] NCRP, "Radiation Protection for Particle Accelerator Facilities: Recommendation of the National Council on Radiation Protection and Measurements", NCRP Report No. 144, 2003.
- [14] N. V. Mokhov and W. Chou (Eds.), "Beam Halo and Scraping", the 7th ICFA Mini-Workshop on High Intensity High Brightness Hadron Beams, Wisconsin, USA, 13-15 September 1999, 3.
- [15] R. M. Ronningen, G. Bollen, and I. Remec, "Estimated Limits on Uncontrolled Beam Losses of Heavy Ions for Allowing Hands-on Maintenance at an Exotic Beam Facility LINAC", Nuclear Technology, 168 (2009), article in press.
- [16] <http://www-linux.gsi.de/~weick/atima>
- [17] <http://www.srim.org/>
- [18] A.A. Golubev, A.V. Kantsyrev, V.E. Luckjashin et al., "Measurement of the energy deposition profile for  $^{238}\text{U}$  ions with specific energy 500 and 950 MeV/u in stainless steel and copper targets", Nucl. Instr. and Meth. in Phys. Res. B 263 (2007) 339.
- [19] <http://ie.lbl.gov/toi/>